Hot workability and microstructure evolution of wire arc additive manufactured 300M steel

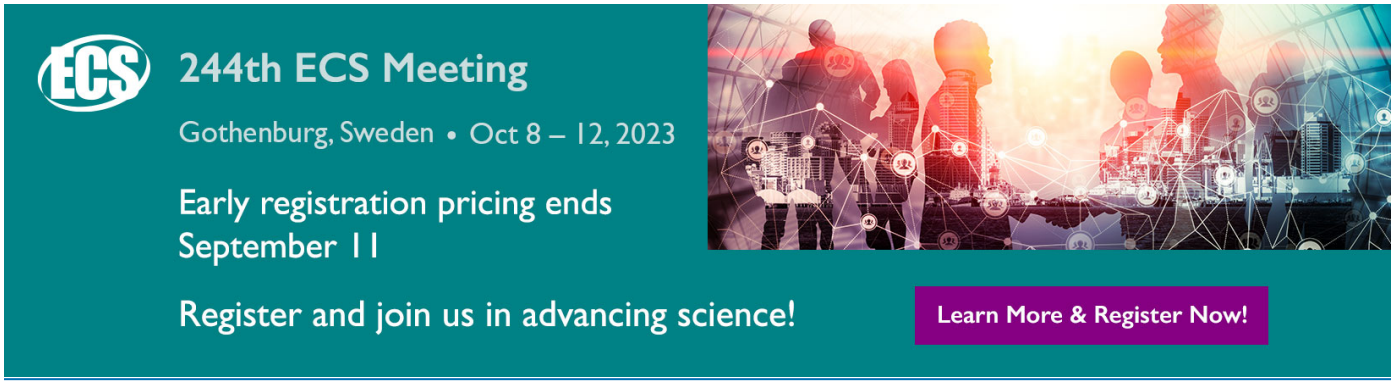

Hot workability and microstructure evolution of wire arc additive manufactured 300M steel

Y B Xiong, D X Wen*, Z Z Zheng and J J Li
* Corresponding author, E-mail: dxwen@hust.edu.cn
State Key Laboratory of Materials Processing and Die & Mould Technology, School of Materials Science and Engineering, Huazhong University of Science and Technology, Wuhan, 430074, P.R. China

Abstract. Wire arc additive manufacturing (WAAM) technology offers a material-saving and efficient method of manufacturing the 300M steel components, but the obtained microstructure and properties hardly reach the level of wrought materials. By combining WAAM technology with forging process, a novel forming process is proposed. The preferred shape pre-forgings are easily prepared, and the number of forging steps significantly decreases. The WAAMed as-cast microstructure also can be transformed into the wrought state by the proposed forming process. The aim of this study is to investigate the hot deformation behavior and microstructure evolution of WAAMed 300M steel under various deformation temperatures and strain rates. The results show that the WAAMed 300M steel exhibits a higher plastic deformation resistance than the wrought 300M steel. With the increase of deformation temperature and strain rate, the difference of flow stress between the WAAMed and wrought 300M steel decreases. The hot deformation activation energy of WAAMed 300M steel is calculated as 374.1 kJ/mol, which is much higher than that of wrought 300M steel (332.3 kJ/mol). The possible processing windows obtained from the hot deformation activation energy maps are 1040-1120 ℃/0.01-10 s^{-1} for the WAAMed 300M steel and 1010-1130 ℃/ 0.1-10 s^{-1} for the wrought 300M steel. The constitutive model considering strain compensation is established to describe the hot deformation behaviors of WAAMed and wrought 300M steel. The high correlation coefficient and low average absolute relative error confirm the suitability of the developed constitutive models for predicting the flow stresses of WAAMed and wrought 300M steel.
Keywords. hot workability; microstructure evolution; wire arc additive manufacturing; 300m steel

1. Introduction

300M steel is a medium carbon low-alloyed steel and widely applied in the aerospace field due to its ultrahigh strength and superior fracture toughness [1]. Hot forging is one of the most common traditional methods for manufacturing high-performance 300M steel parts [2]. Generally, the manufacturing process of 300M steel parts is divide into three steps: blank making, pre-forging and final forging [3]. Some disadvantages, such as long manufacturing period, low material utilization rate and high tooling costs are hardly avoided in the conventional manufacturing process. Wire arc additive manufacturing (WAAM) technology is a layer-by-layer deposition forming technology that offers a material-saving and efficient method of manufacturing the 300M steel components [4]. However, the microstructure and properties of as-deposited materials hardly reach the level of wrought materials [5]. Therefore, a novel process by combining WAAM technology with forging process is proposed. It offers the possibility of creating near-net shape pre-forgings, reducing the number of forging steps, and obtaining the desired microstructure and properties [6].

In addition to WAAM parameters, hot deformation parameters also play an important role in the defect elimination and microstructure evolution [7]. Thus, the study of hot deformation behavior of WAAMed material is significant for achieving a preferred match between WAAM technology and hot forging process. Recently, some studies have been reported on the hot deformation behavior and microstructure evolution of AMed materials. Bambach et al. [8] studied the differences in the hot deformation behavior of selective laser melted (SLMed), directed energy deposited (DEDed) and wrought Ti-6Al-4V alloy. They found that the SLMed and DEDed Ti-6Al-4V alloys show the low activation energy and fast globularization rate compared to wrought alloy, due to the low fraction of β phase and random arrangement of α phase. Zhou et al. [9] found that the WAAMed 2219 Al alloy exhibits the high flow stress and activation energy compared to as-cast and wrought samples. The main reason is that a large number of θ' phases present in the WAAMed 2219 Al alloy impede the dislocation movement, resulting in the increased deformation resistance. Lan et al. [10] investigated the effect of anisotropic microstructure on the hot deformation behavior of WAAMed IN718 alloy. They found that the uniaxial compressed samples of different orientations exhibit the similar flow stress-strain curves under different hot deformation conditions, and a more uniform microstructure with the equiaxed fine recrystallized grains could be obtained when the compression direction is perpendicular to the building direction. So far, most of the previous studies have focused on the hot deformation behavior and microstructure evolution of additively manufactured titanium alloys, aluminum alloys and superalloys. However, the studies on the hot deformation behavior and microstructure evolution of WAAMed 300M steel are seldom.

In this study, the hot deformation behavior and microstructure evolution of WAAMed and wrought 300M steel are investigated through hot compression testing under deformation temperatures of 920-1160 ℃ and strain rates of 0.01-10 s^{-1}. A comparative analysis of hot deformation behavior and microstructure evolution of WAAMed and wrought 300M steel is carried out. Moreover, the constitutive model considering strain compensation is established to describe the flow stresses of WAAMed and wrought 300M steel.

2. Materials and methods

2.1. Sample preparation

The 300M steel samples were fabricated by WAAM technology on the Fronius CMT 4000 Advanced machine. The diameter of 300M steel wire was 1.2mm, and the 300M steel plate with a thickness of 20 mm was used as the substrate. Prior to deposition, the substrate surface was polished and cleaned to remove the oxide layer and oil. The optimized WAAM process parameters are presented as following: wire feed speed 6.5 m/min, deposition speed 0.42 m/min, shielding gas 80%Ar+20%CO_2, gas flow rate 20 L/min, and interlayer temperature 200 ℃. The WAAMed 300M steel block with the length of 100 mm, the width of 40 mm and the height of 60 mm was fabricated by using the round-trip deposition strategy. The chemical compositions of the 300M steel substrate and WAAMed block are presented in table 1. The cylindrical samples with the dimension of $\Phi 8 \times 12$ mm were machined from the middle area of the WAAMed block, as shown in figure 1.

Table 1. Chemical compositions of the 300M steel substrate and WAAMed block (wt. %).

300M steel	C	Si	Mn	S	P	Cr	Ni	Cu	V	Mo
Substrate	0.38	1.8	0.71	0.01	0.01	0.83	1.93	0.15	0.07	0.38
WAAMed block	0.34	2.1	0.73	0.007	0.008	0.92	2.23	0.17	0.07	0.41

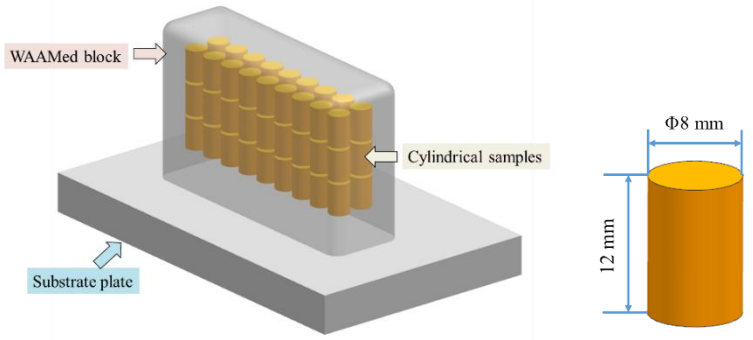

(a) (b)

Figure 1. (a) The location of the cylindrical samples in the WAAMed block; (b) the dimensions of the cylindrical samples.

2.2. Hot compression testing

The hot compression tests were carried out at temperatures from 920 ℃ to 1160 ℃, and strain rates from 0.01 s^{-1} to 10 s^{-1}. The WAAMed cylindrical samples were first heated to 1200 ℃ and soaked for 180 s to guarantee homogeneous temperature. Then, these samples were cooled to the deformation temperature, soaked for 120 s and deformed to a true strain of 0.8. After deformation, all samples were instantly water quenched to preserve the deformed austenite grain boundaries. For comparison, the wrought cylindrical samples were also subjected to hot compression tests under the same deformation conditions for the WAAMed samples.

2.3. Material characterization

All samples were cut along the compression direction, and their cross-sections were prepared according to the standard procedures for microstructure analysis. The saturated picric acid etchant was used to reveal the prior austenite grain boundaries with the etching time of 5 min. After etching, the Zeiss Axiovert 200MAT optical microscope (OM) and the FEI sirion scanning electron microscope (SEM) were employed to observe the microstructure.

3. Results and discussion

3.1. Initial microstructures

Figure 2 shows the initial microstructures of WAAMed and wrought 300M steel. As shown in figure 2(a), there are no cracks observed in the WAAMed 300M steel, and the microstructure of WAAMed 300M steel exhibits the columnar dendrites with the preferred growth orientation along the deposition direction due to the high temperature gradient. The average dendrite spacing is 12.8 μm. As shown in figure 2 (b), the microstructure of wrought 300M steel presents the equiaxed grains with the average grain size of 72.4 μm.

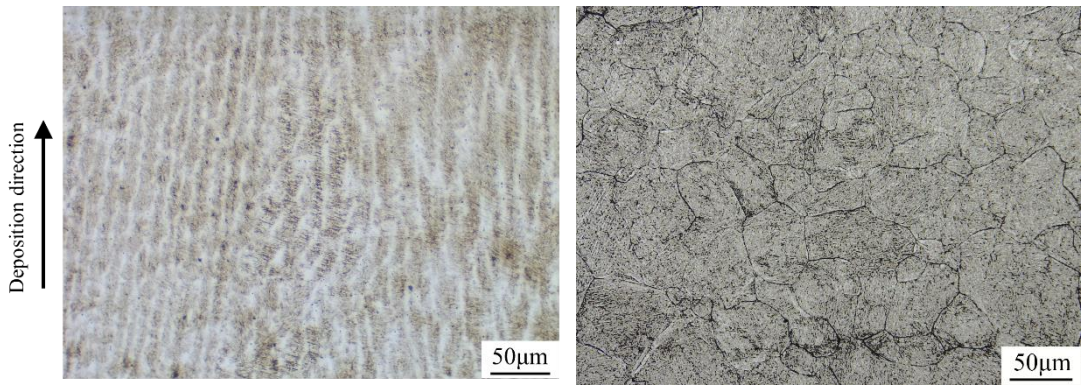

(a) (b)

Figure 2. Initial microstructures of: (a) WAAMed 300M steel; (b) wrought 300M steel.

3.2. Stress-strain curves

The selected stress-strain curves of WAAMed and wrought 300M steel are shown in figure 3. The solid line represents the WAAMed 300M steel and the dashed line represents the wrought 300M steel. As shown in figure 3(a), the flow stress of WAAMed 300M steel is significantly higher than that of wrought 300M steel under the strain rate of 0.01 s^{-1}. On the one hand, the microstructure of WAAMed 300M steel with small dendrite spacing provides more grain boundaries for strengthening the material, leading to the increase of flow stress. On the other hand, the repeated heating treatment during the WAAM process promotes the precipitation of carbides [11]. During hot deformation, these carbides impede dislocation movement, which leads to the increase of flow stress. Additionally, under the strain rate of 0.01 s^{-1}, the difference in flow stress between the WAAMed and wrought 300M steel decreases with the increase of deformation temperature. As the deformation temperature increases, these carbides gradually dissolve and the pinning effect of carbides weakens, resulting in the decrease of the difference in flow stress between the WAAMed and wrought 300M steel. As shown in figure 3(b), under the strain rate of 10 s^{-1}, the flow stress of WAAMed 300M steel is slightly higher than that of wrought 300M steel at the early deformation stage. As the strain increases, the flow stress of WAAM 300M steel tends to be consistent with that of wrought 300M steel. Some undissolved carbides can act as nucleation sites of dynamic recrystallization (DRX) grains, which promotes the progress of DRX. Therefore, the flow stress of WAAMed 300M steel decreases and tends to be consistent with the flow stress of wrought 300M steel.

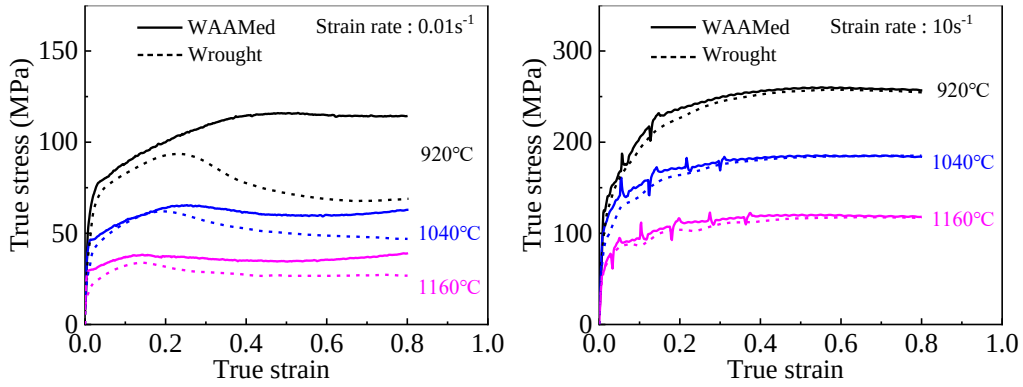

Figure 3. Selected stress-strain curves of WAAMed and wrought 300M steel under different temperatures and strain rates of: (a) 0.01s^{-1}; (b) 10s^{-1}.

3.3. Hot deformation behavior and constitutive model

The hot deformation activation energy (Q) describes the activation barrier that needs to be overcome for the atomic transition, and it represents the hot workability of the material. According to the Arrhenius equation [12], Q can be determined as:

$$Q=R\left\{\frac{\partial \ln \dot{\varepsilon}}{\partial \ln\left[\sinh(\alpha\sigma)\right]}\right\}_T\left\{\frac{\partial \ln\left[\sinh(\alpha\sigma)\right]}{\partial(1/T)}\right\}_{\dot{\varepsilon}} \tag{1}$$

where $\dot{\varepsilon}$ is the strain rate, T is the deformation temperature, α is the materials constant, R is the gas constant.

Base on equation (1), the Q values for WAAMed and wrought 300M steel are calculated, and the Q maps are plotted in figure 4. As shown in figure 4, the Q value for WAAMed 300M steel varies from 321.9 to 439.8 kJ/mol with an average value of 374.1 kJ/mol, and the Q value for wrought 300M steel varies from 242.8 to 379.0 kJ/mol with an average value of 332.3 kJ/mol. Overall, the WAAMed 300M steel shows the higher Q value than that of wrought 300M steel, and this phenomenon becomes more obvious when the deformation temperature is relatively low (T < 980 ℃). It indicates that the WAAMed 300M steel is more difficult to be processed than the wrought 300M steel under low deformation temperature. The differences in Q values of WAAMed and wrought 300M steel could be attributed to

the distinct initial microstructures and grain sizes. Moreover, the Q map is beneficial to identify the hot processing window for the materials. As the Q describes the underlying deformation mechanisms associated with the microstructural development, so the constant value of Q indicates the similar microstructural evolution [13]. According to Wen [14] and Sun [15], the potential optimal processing window can be considered as the domain with nearly constant and relatively high Q value in the Q map. In Fig. 4(a), the region with low variation of Q is located at the high temperature. As shown in Fig. 4(b), the Q values exhibit almost a plateau under the high deformation temperature and strain rate. Therefore, the possible processing windows are 1040-1120 ℃/0.01-10 s^{-1} for the WAAMed 300M steel and 1010-1130 ℃/ 0.1-10 s^{-1} for the wrought 300M steel. However, it is noted that only relying on the Q map, the processing window optimization and microstructure control might not be realized precisely.

The Arrhenius type constitutive model considering strain compensation is established to describe the flow curves of WAAMed and wrought 300M steel. The flow stress can be calculated as:

$$\sigma=\frac{1}{\alpha}\ln\left\{\left(\frac{\dot{\varepsilon}}{A}\exp\left(\frac{Q}{RT}\right)\right)^{1/n}+\left[\left(\frac{\dot{\varepsilon}}{A}\exp\left(\frac{Q}{RT}\right)\right)^{2/n}+1\right]^{1/2}\right\} \tag{2}$$

where A and n are the material parameters. The relationships between these material parameters (Q, $\ln A$, n and α) and strain (ε) can be summarized as,

for WAAMed 300M steel:

$$\begin{pmatrix} Q \\ \ln A \\ n \\ \alpha \end{pmatrix}=\begin{pmatrix} 324.184 & 569.329 & -2395.371 & 5321.327 & -6178.551 & 2866.019 \\ 28.662 & 34.878 & -126.777 & 269.518 & -329.603 & 165.323 \\ 5.812 & -7.573 & 37.326 & -109.345 & 142.959 & -65.834 \\ 0.013 & -0.025 & 0.060 & -0.054 & 0.002 & -0.014 \end{pmatrix}\begin{pmatrix} 1 \\ \varepsilon \\ \varepsilon^2 \\ \varepsilon^3 \\ \varepsilon^4 \\ \varepsilon^5 \end{pmatrix} \tag{3}$$

for wrought 300M steel:

$$\begin{pmatrix} Q \\ \ln A \\ n \\ \alpha \end{pmatrix}=\begin{pmatrix} 329.591 & 908.013 & -5014.081 & 9983.253 & -8969.282 & 3043.043 \\ 28.478 & 74.771 & -415.802 & 812.841 & -709.221 & 231.412 \\ 5.355 & 3.552 & -49.172 & 114.658 & -106.562 & 35.506 \\ 0.016 & -0.057 & 0.224 & -0.413 & 0.365 & -0.125 \end{pmatrix}\begin{pmatrix} 1 \\ \varepsilon \\ \varepsilon^2 \\ \varepsilon^3 \\ \varepsilon^4 \\ \varepsilon^5 \end{pmatrix} \tag{4}$$

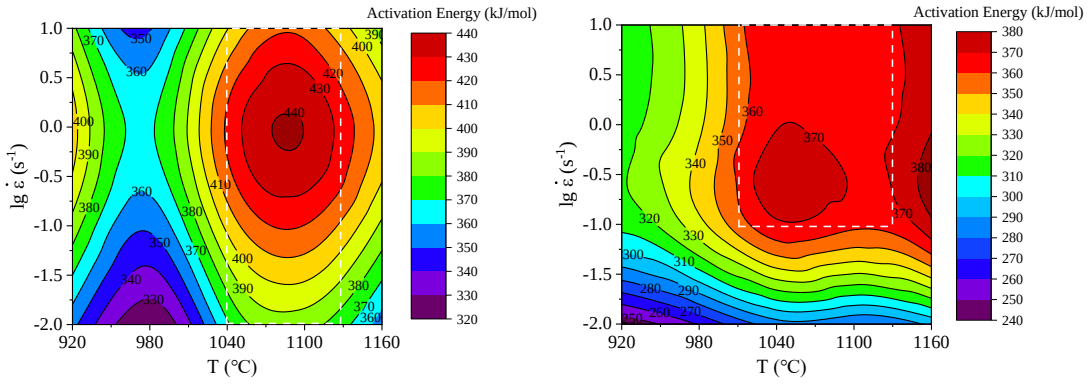

(a) (b)

Figure 4. The hot deformation activation energy maps of (a) WAAMed and (b) wrought 300M steel at peak stress.

The comparisons between the experimental and calculated stresses for WAAMed and wrought 300M steel under various deformation parameters are shown in figure 5. It can be seen that the experimental and calculated stresses for both materials show the excellent agreement.

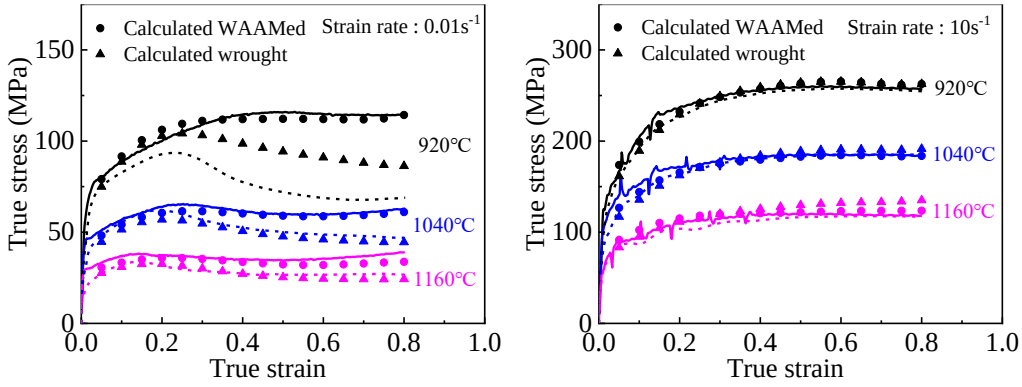

(a) (b)

Figure 5. Comparisons between the experimental and calculated stresses for WAAMed and wrought 300M steel at the strain rates of: (a) 0.01 s^{-1}; (b) 10 s^{-1}.

In order to further evaluated the accuracy of the Arrhenius type model for WAAMed and wrought 300M steel, the correlation coefficient (R) and average absolute relative error ($AARE$) between the experimental and calculated stresses are determined by the following equations,

$$R = \frac{\sum_{i=1}^{N}\left(E_i - \overline{E}\right)\left(C_i - \overline{C}\right)}{\sqrt{\sum_{i=1}^{N}\left(E_i - \overline{E}\right)^2 \sum_{i=1}^{N}\left(C_i - \overline{C}\right)^2}} \tag{5}$$

$$AARE(\%) = \frac{1}{N}\sum_{i=1}^{N}\left|\frac{E_i - C_i}{E_i}\right| \tag{6}$$

where E_i and C_i are the experimental and calculated stresses, $\overline{E}$ and $\overline{C}$ are the average values of E_i and C_i respectively, and N is the total amount of the experimental data.

As shown in figure 6(a), the values of R and $AARE$ for WAAMed 300M steel are determined as 0.997 and 4.03%, respectively. Moreover, the 90% of the value points are concentrated in the scatter band of $\pm$ 8 MPa. As shown in figure 6(b), the values of R and $AARE$ for wrought 300M steel are determined as 0.987 and 6.79%, respectively. The value points are mainly located in the scatter band of $\pm$ 18 MPa. These results indicate that the developed constitutive model can well predict the flow stresses of WAAMed and wrought 300M steel. Additionally, these results also show that the WAAMed materials can be modelled in the same way as the wrought materials, which is beneficial for the finite simulation analysis of hybrid manufacturing process of WAAMed and wrought materials.

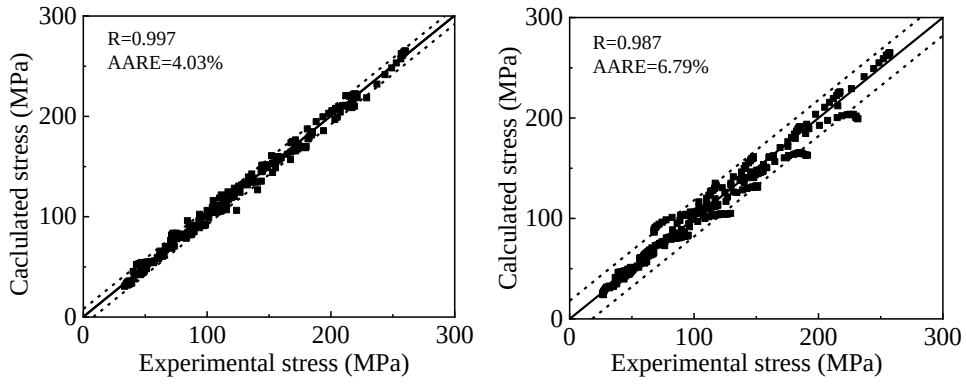

(a) (b)

Figure 6. Correlations between the experimental and calculated stresses of: (a) WAAMed 300M steel; (b) wrought 300M steel.

3.4. Microstructure evolution

Figure 7 shows the microstructures of WAAMed and wrought 300M steel after deformation at different deformation parameters. As shown in figure 7(a) and 7(d), under the deformation temperature of 920 ℃ and strain rate of 10 s^{-1}, there are some elongated grains in the microstructure of both materials, and some fine DRX grains are distributed around the elongated grain boundaries. It indicates that the incomplete DRX takes place in the WAAMed and wrought 300M steel under the low deformation temperature and high strain rate. In figure 7 (b) and 7(e), the deformation parameters of WAAMed and wrought 300M steel are 1040 ℃/0.01 s^{-1} and 1040 ℃/1 s^{-1}, respectively, which are located in the optimal processing windows obtained from the hot deformation activation energy maps. Under these deformation parameters, the materials undergo the complete DRX and the microstructures consist of uniform and fine equiaxed grains. The average grain sizes of WAAMed and wrought 300M steel are 30.8 and 32.2 μm. However, when the deformation temperature increases to 1160 ℃, a significant growth of the DRX grains occurs in WAAMed and wrought 300M steel, as shown in figure 7(c) and 7(f). It is noted that the average grain size of WAAMed 300M steel (124.5 μm) is much larger than that of wrought 300M steel (69.8 μm). Overall, these results are in accordance with the processing windows obtained by the hot deformation activation energy maps of WAAMed and wrought 300M steel.

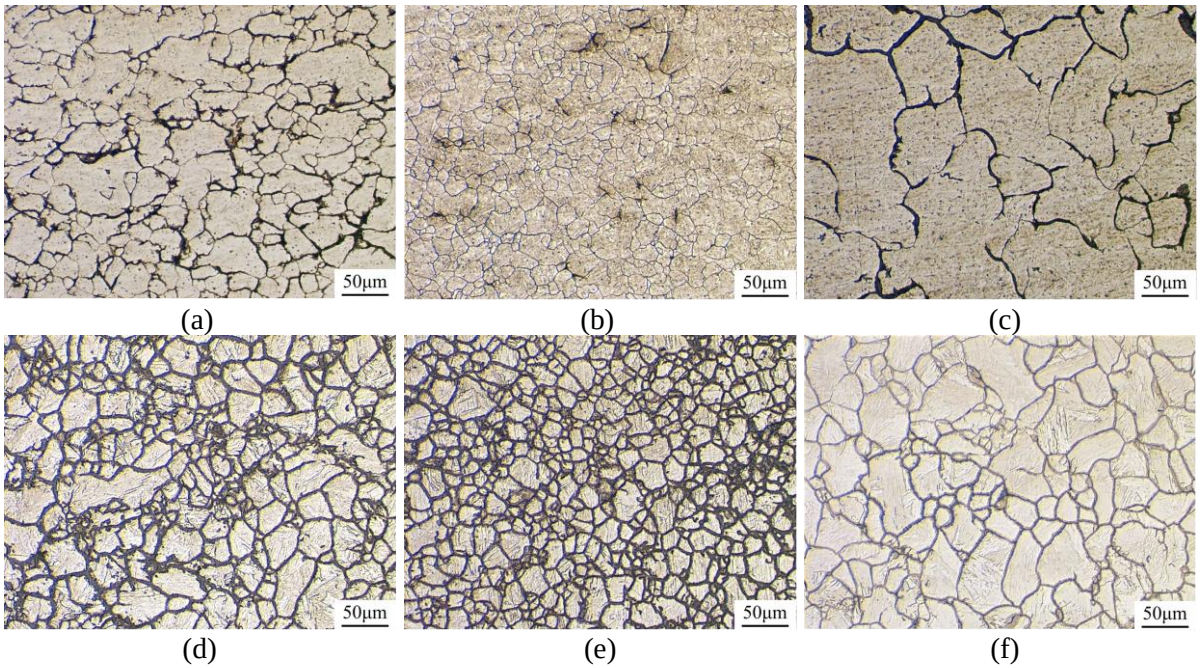

Figure 7. Microstructures of 300M steel under different deformation parameters: (a) WAAMed, 920 ℃ and 10 s^{-1}; (b) WAAMed, 1040 ℃ and 0.01 s^{-1}; (c) WAAMed, 1160 ℃ and 0.01 s^{-1}; (d) wrought, 920 ℃ and 10 s^{-1}; (e) wrought, 1040 ℃ and 1 s^{-1}; (f) wrought, 1160 ℃ and 0.01 s^{-1}.

4. Conclusions

In this work, the comprehensive comparison of hot deformation behaviour and microstructure evolution of WAAMed and wrought 300M steel is investigated. Based on the investigation results, some important conclusions can be summarized as:

(1) The flow stress of WAAMed 300M steel is higher than that of wrought 300M steel due to the distinct initial microstructures and grain sizes. With the increase of deformation temperature and strain rate, the difference of flow stress between the WAAMed and wrought 300M steel decreases.

(2) The hot deformation activation energy of WAAMed 300M steel is 374.1 kJ/mol, which is higher than that of wrought 300M steel (332.3 kJ/mol). The preferred processing windows obtained from the hot deformation activation energy maps are 1040-1120 ℃/0.01-10 s^{-1} for the WAAMed 300M steel and 1010-1130 ℃/ 0.1-10 s^{-1} for the wrought 300M steel. Under these deformation parameters, the materials undergo the complete DRX and the microstructures consist of uniform and fine

equiaxed grains. The average grain sizes of WAAMed and wrought 300M steel are kept in 30.8 and 32.2 μm, respectively.

(3) The constitutive model considering strain compensation is established to describe the hot deformation behaviors of WAAMed and wrought 300M steel. The high R and low $AARE$ confirm the suitability of the developed constitutive model for predicting the flow stresses of WAAMed and wrought 300M steel.

References

[1] Wen D X, Yue T Y, Xiong Y B, Wang K, Wang J K, Zheng Z Z and Li J J 2021 *Mater. Sci. Eng. A.* **803** 140491
[2] Xue X W, Wang C X, Li Y, Han S and Yuan W H 2019 *Key Eng. Mater.* **815** 99-106
[3] Li C M, Huang L, Zhao M J, Zhang X T, Li J J and Li P C 2020 *Mater. Sci. Eng. A.* **797** 139925
[4] Liu F G, Lin X, Shi J, Zhang Y J, Bian P Y, Li X and Hu Y L 2019 *Addit. Manuf.* **29** 100795
[5] Xiong Y B, Wen D X, Zheng Z Z and Li J J 2022 *Mater. Sci. Eng. A.* **831** 142351
[6] Bambach M, Sizova I, Sydow B, Hemes S and Meiners F 2022 *J. Mater. Process. Technol.* **282** 116689
[7] Wen D X, Long P, Li J J, Huang L and Zheng Z Z 2019 *Vacuum* **173** 109131
[8] Bambach M, Sizova I, Szyndler J, Bennett J, Hyatt G, Cao J, Papke T and Merklein M 2021 *J. Mater. Process. Technol.* **288** 116840
[9] Zhou Y H, Lin X, Kang N, Wang Z N, Tan H and Huang W D 2021 *J. Alloys Compd.* **865** 158949
[10] Lan B, Wang Y P, Liu Y H, Hooper P, Hopper C, Zhang G D, Zhang X J and Jiang J 2021 *Mater. Sci. Eng. A.* **823** 141733
[11] Jing G Y and Wang Z M 2021 *Addit. Manuf.* **38** 101831
[12] Sellars C M and McTegart W J 1966 *Acta Metall.* **14** 1136-38
[13] Son K T, Kim M H, Kim S W, Lee J W and Hyun S K 2018 J. Alloys Compd. 740 96-108
[14] Wen D X, Lin Y C, Li H B, Chen X M, Deng J and Li L T 2014 *Mater. Sci. Eng. A.* **591** 183-92
[15] Sun Y, Wan Z P, Hu L X and Ren J S 2015 *Mater. Des.* **86** 922-32

Acknowledgments

The authors gratefully thank the financial support by National Key R&D Program of China (No. 2018YFB1106501), National Natural Science Foundation of China (No. 51905190, 52075197), and the Fundamental Research Funds for the Central Universities, China (No. 2019kfyXJJS001).